Liquid Crystals
Publication details, including instructions for authors and subscription information:
http://www.informaworld.com/smpp/title~content=t713926090

Mesomorphic 4'-functionalized 6'-phenyl-2,2'-bipyridines: tridentate ligands for organopalladium mesogens

Francesco Neve; Mauro Ghedini; Oriano Francescangeli; Sebastiano Campagna

Online publication date: 06 August 2010

To cite this Article Neve, Francesco , Ghedini, Mauro , Francescangeli, Oriano and Campagna, Sebastiano(1998) 'Mesomorphic 4'-functionalized 6'-phenyl-2,2'-bipyridines: tridentate ligands for organopalladium mesogens', Liquid Crystals, 24: 5, 673 — 680
To link to this Article: DOI: 10.1080/026782998206777
URL: http://dx.doi.org/10.1080/026782998206777

LIQUID CRYSTALS, 1998, VOL. 24, NO. 5, 673–680

Mesomorphic 4′-functionalized 6′-phenyl-2,2′-bipyridines: tridentate ligands for organopalladium mesogens

by FRANCESCO NEVE*, MAURO GHEDINI
Dipartimento di Chimica, Università della Calabria,
I-87030 Arcavacata di Rende (CS), Italy

ORIANO FRANCESCANGELI
Dipartimento di Scienze dei Materiali e della Terra, Sezione Fisica,
Università di Ancona, Via Brecce Bianche, I-60131 Ancona, Italy

and SEBASTIANO CAMPAGNA
Dipartimento di Chimica Inorganica, Chimica Analitica e Chimica Fisica,
Università di Messina, via Sperone 31, I-98166 Messina, Italy

(*Received 17 October 1997; accepted 10 December 1997*)

A novel series of 6′-phenyl-2,2′-bipyridines (HL-*n*) substituted in the 4′ position with promesogenic functional groups has been prepared. The materials are strongly luminescent and display nematic mesomorphism. The HL-*n* behave as *C*,*N*,*N*-tridentate, cyclometallating ligands leading to [Pd(L-*n*)Cl] derivatives. Metal co-ordination promotes a considerable stabilization of the crystal phase, forcing mesophases to become metastable. All [Pd(L-*n*)Cl] species indeed exhibit a monotropic mesophase either nematic or smectic A in character depending on the chain length of the substituents on the central pyridine unit.

1. Introduction

In the search for novel mesogenic materials, the need for structural variation has recently prompted the rapid growth in the number of metallomesogens (metal-containing liquid crystals), an area of research developed mainly in the last decade [1–3]. The early approach to the design of metallomesogens consisted in making use of well-known organic mesogens containing potential donor atoms. Species such as *p*-substituted cyanobiphenyls attracted the attention of synthetic chemists owing to the relevant optical properties of the organic materials [4] and mesomorphic transition metal adducts of both class A and B (figure 1) have been easily obtained [5]. However, it soon became clear that: (i) even non-mesogenic ligands could lead to liquid crystal behaviour upon metal co-ordination and (ii) the range of ligands able to yield metallomesogens could expand well beyond that already at hand. In both cases, it was just a matter of will, luck, and time.

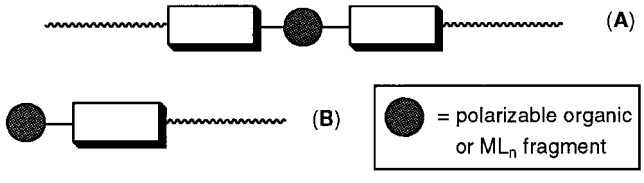

Figure 1. The most commonly seen icons for a calamitic mesogen are symmetric (A) or asymmetric (B) rods.

Tridentate ligands are rare among those involved in the formation of mesogenic complexes. They include a *N*-substituted triazacyclononane [6], a 4-substituted pyridinediyl-2,6-dimethanolate [7], and a 1,3,5-triketone [8]. None of them is mesomorphic individually, but the resulting metal complexes show thermotropic behaviour. The more familiar 2,2′:6′,2″-terpyridine (terpy) ligand has also been functionalized with alkyl groups in order to obtain lyotropic complexes. Bis(R-terpy) ruthenium and rhodium species which exibit lyomesophases have also been isolated [9].

We have recently approached a new class of substituted 6′-phenyl-2,2′-bipyridines that behave as *C*,*N*,*N*-tridentate ligands and which can act as luminophores [10, 11]. The otherwise wide 6′-phenyl-2,2′-bipyridine skeleton can be made roughly rod-like through functionalization at the 4-position of the central pyridine unit. Functionalities included 4-alkoxyphenyl ($m = 0$) and (4-alkoxybenzoyloxy)phenyl ($m = 1$) groups [10, 11] (figure 2).

*Author for correspondence.

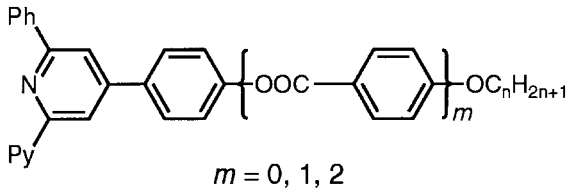

Figure 2. General structure of 4-functionalized 6′-phenyl-2,2′-bipyridines.

However, mesomorphism only arises when two benzoate ester groups ($m = 2$) are incorporated into the core of the mesogen. Here we report on a short series of diester derivatives of 6′-phenyl-2,2′-bipyridine (HL-*n*) and their thermal, photophysical, and complexation behaviour. A preliminary report of part of this work appeared earlier [10].

2. Experimental

2.1. *Materials and methods*

1-Phenyl-3-(4-hydroxyphenyl)propen-1-one (Lancaster), ammonium acetate, 98% (Lancaster), 1,3-dicyclohexylcarbodiimide (DCC) (Aldrich), and 4-pyrrolidinopyridine (PPy) (Aldrich) were used as received. 4-(4-Alkoxybenzoyloxy)benzoic acids (**2-*n***) were prepared by standard methods starting from commercially available 4-alkoxybenzoic acids (Aldrich) and benzyl 4-hydroxybenzoate (Lancaster). 1-(2-Pyridinylcarbonyl)-pyridinium iodide [12] was obtained according to a recently published procedure. [$(PhCN)_2PdCl_2$] was prepared according to the literature [13].

The products were characterized by analytical, spectroscopic, optical, calorimetric and diffractometric methods. The purity and chemical structure of intermediates and final products were investigated by IR (Perkin Elmer System 2000 FT spectrophotometer) and NMR (Bruker AC300 with tetramethylsilane as internal standard) spectroscopy. Elemental analyses were performed using a Perkin Elmer 2400 microanalyser.

Absorption spectra were recorded using a Kontron Uvikon 860 spectrophotometer. Luminescence spectra and lifetimes were obtained with a Perkin Elmer LS-5B spectrofluorimeter equipped with a red-sensitive Hamamatsu R928 photomultiplier and with an Edinburgh FL-900 single-photon-counting spectrometer, respectively. Luminescence spectra were corrected for photomultiplier response by calibrating the spectrofluorimeter with a standard lamp. Luminescence quantum yields were measured at room temperature (20°C) using the optically dilute method [14], employing anthracene in degassed ethanol solution as a quantum yield standard ($\Phi = 0{\cdot}27$ [15]). For the luminescence measurements at 77 K, we used butyronitrile because of the transparency of the matrix. Experimental errors were as follows: absorption maxima, 2 nm; emission maxima, 4 nm; molar absorption coefficients, 10%; emission lifetimes, 10%; emission quantum yields, 10%.

Phase transitions and assignments for the materials were determined by thermal optical microscopy by means of a Zeiss Axioskop polarizing microscope equipped with a heating stage and a temperature control unit. Transition temperatures and enthalpies were determined by differential scanning calorimetry (DSC) using a Perkin Elmer DSC7 calorimeter operating at a scanning rate of 10°C min^{-1}. Materials were sealed in aluminium pans and measurements were carried out keeping a dry nitrogen atmosphere in the furnace.

X-ray diffraction (XRD) experiments on powder samples were performed using the INEL CPS 120 powder diffractometer as described previously [16]. A stationary magnetic field of 0·3 T normal to the incident beam was also used to align the samples in the nematic mesophase.

2.2. *Synthesis*

The synthetic route to HL-*n* ligands and [Pd(L-*n*)Cl] derivatives is illustrated in the scheme.

2.2.1. *4′-(4-Hydroxyphenyl)-6′-phenyl-2,2′-bipyridine (**1**)*

A 10 fold excess of ammonium acetate was added to a mixture of equimolar amounts of 1-phenyl-3-(4-hydroxyphenyl)propen-1-one (0·724 g) and 1-(2-pyridinylcarbonyl)pyridinium iodide (1·008 g) in methanol (25 cm^3). The mixture was then heated at reflux for 6 h. Overnight cooling of the resulting dark green solution to room temperature afforded an off-white fluffy solid, which was filtered off, washed with cold methanol and vacuum dried. Another crop of pure product was obtained upon further heating of the mother liquor under reflux for 5 h and subsequent work-up. This procedure is to be preferred to a single heating process for a longer time. Overall yield 0·595 g (57%), m.p. 272°C. Found: C, 81·32; H, 4·72; N, 8·40. Calc. for $C_{22}H_{16}N_2O$: C, 81·46; H, 4·97; N, 8·63%. ^{1}H NMR δH [$(CD_3)_2CO$, 300 MHz] 8·63 (br d, 1 H, H-6), 8·62 (d, 1 H, H-3), 8·60 (d, 1 H, H-3′), 8·26 (d, 2 H, H-2″, 6″), 8·11 (d, 1 H, H-5′), 7·89 (ddd, 1 H, H-4), 7·46 (m, 3 H, H-3″, 4″, 5″), 7·37 (m, 1 H, H-5). Other signals 8·84 (s, 1 H, OH), 7·77 (d, 2 H), 6·96 (d, 2 H).

2.2.2. *HL-*n *ligands*

The following procedure is typical for the preparation of compounds HL-*n* ($n = 6$, 8, 12).

2.2.2.1. *4-{4-[4-Hexyloxybenzoyloxy)benzoyloxy]phenyl}-6′-phenyl-2,2′-bipyridine (HL-6)*. A mixture of 4-(4-hexyloxybenzoyloxy)benzoic acid (**2**–**6**) (0·264 g, 0·77 mmol), compound **1** (0·250 g, 0·77 mmol), DCC (0·159 g, 0·77 mmol), and PPy (0·011 g, 0·077 mmol) in dichloromethane (60 ml) was stirred at room temperature for

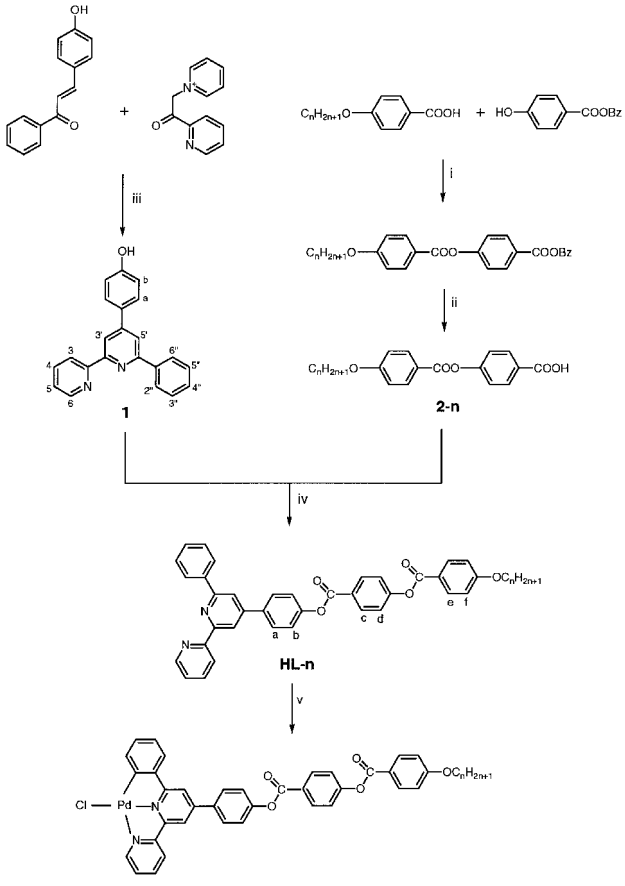

Scheme. Synthetic route to HL-*n* ligands and organopalladium derivatives. Reagents and conditions: (i) DCC, PPy, CH_2Cl_2; (ii) H_2, 10% Pd/C, CH_2Cl_2; (iii) [NH_4][OAc], MeOH; (iv) DCC, PPy, CH_2Cl_2; (v) [$Pd(PhCN)_2Cl_2$], benzene-MeOH.

24 h. After removing a white solid by filtration, the colourless filtrate was consecutively washed with water ($2 \times 20\,cm^3$), 5% acetic acid ($2 \times 20\,cm^3$), and water ($2 \times 20\,cm^3$). The organic phase was dried over Na_2SO_4 and the solvent removed *in vacuo*. The crude residue (0·420 g) was then purified by column chromatography (SiO_2, CH_2Cl_2/5%MeOH) followed by repeated crystallization (CH_2Cl_2/*n*-hexane) at −20°C. The product was obtained as a pure white solid in 26% yield (0·130 g). More product was also recovered mixed with unidentified by-products, but it was difficult to purify. Found: C, 77·80; H, 5·62, N, 4·15. Calc. for $C_{42}H_{36}N_2O_5$: C, 77·76; H, 5·59; N, 4·32%. IR *v* (Nujol mull)/cm^{-1} 1745, 1729 (COO). ^{1}H NMR δ_H ($CDCl_3$, 300 MHz) 8·73 (br d, 1 H, H-6), 8·69 (d, 1 H, H-3), 8·65 (s, 1 H, H-3′), 8·21 (d, 2 H, H-2″, 6″), 8·00 (br s, 1 H, H-5′), 7·89 (m, 1 H, H-4), 7·57–7·47 (m, 3 H, H-3″, 4″, 5″), 7·26 (m, 1 H, H-5). Other signals: δ 8·32 (d, 2 H, H-c), 8·16 (d, 2 H, H-e), 7·91 (d, 2 H, H-a), 7·39 (d, 4 H, H-b + H-d), 6·99 (d, 2 H, H-f), 4·06 (t, 2 H, OCH_2), 1·82 (m, 2 H, OCH_2CH_2), 1·49–1·34 [m, 6 H, $(CH_2)_3$], 0·91 (t, 3 H, CH_3). δ_C ($CDCl_3$, 75 MHz) 164·3, 163·9, 157·3, 156·5, 156·4, 155·6, 151·7, 149·4, 149·1, 139·5, 136·8, 136·6, 132·4, 131·8, 129·1, 128·7, 128·4, 128·3, 127·1, 126·8, 123·8, 122·3, 122·1, 121·5, 121·1, 118·3, 117·5, 114·5, 68·4, 31·5, 29·1, 25·6, 22·5, 13·9.

2.2.2.2. *4-{4-[4-Octyloxybenzoyloxy)benzoyloxy]phenyl}-6′-phenyl-2,2′-bipyridine (HL-8)*. Reaction time, 36 h. Yield, 39%. Found: C, 77·79; H, 5·96; N, 3·99. Calc. for $C_{44}H_{40}N_2O_5$: C, 78·08; H, 5·96; N, 4·14%. IR *v* (Nujol mull)/cm^{-1} 1732 (COO). ^{1}H NMR δ_H ($CDCl_3$, 300 MHz) 8·72 (br d, 1 H, H-6), 8·69 (d, 1 H, H-3), 8·66 (d, 1 H, H-3′), 8·22 (d, 2 H, H-2″, 6″), 7·99 (d, 1 H, H-5′), 7·87 (ddd, 1 H, H-4), 7·52 (m, 3 H, H-3″, 4″, 5″), 7·35 (m, 1 H, H-5). Other signals: δ 8·32 (d, 2 H, H-c), 8·16 (d, 2 H, H-e), 7·90 (d, 2 H, H-a), 7·39 (d, 4 H, H-b + H-d), 6·99 (d, 2 H, H-f), 4·05 (t, 2 H, OCH_2), 1·82 (m, 2 H, OCH_2CH_2), 1·30 [m, 10 H, $(CH_2)_5$], 0·90 (t, 3 H, CH_3). δ_C ($CDCl_3$, 75 MHz) 164·2, 163·9, 157·3, 156·5, 156·4, 155·6, 151·7, 149·4, 149·1, 139·5, 136·7, 136·6, 132·4, 131·8, 129·1, 128·7, 128·4, 127·1, 126·8, 123·7, 122·3, 122·1, 121·5, 121·1, 118·3, 117·5, 114·5, 68·5, 31·8, 29·3, 29·2, 29·1, 26·0, 22·6, 14·0.

2.2.2.3. *4-{4-[4-Dodecyloxybenzoyloxy)benzoyloxy]-phenyl}-6′-phenyl-2,2′-bipyridine (HL-12)*. Reaction time, 36 h. Yield, 32%. Found: C, 79·08; H, 6·70; N, 4·58. Calc. for $C_{48}H_{48}N_2O_5$: C, 78·66; H, 6·60; N, 3·82%. IR *v* (Nujol mull)/cm^{-1} 1732 (COO). ^{1}H NMR δ_H ($CDCl_3$, 300 MHz) 8·73 (br d, 1 H, H-6), 8·70 (d, 1 H, H-3), 8·66 (d, 1 H, H-3′), 8·22 (d, 2 H, H-2″, 6″), 8·00 (d, 1 H, H-5′), 7·88 (ddd, 1 H, H-4), 7·58–7·47 (m, 3 H, H-3″, 4″, 5″), 7·35 (m, 1 H, H-5). Other signals: δ 8·32 (d, 2 H, H-c), 8·16 (d, 2 H, H-e), 7·90 (d, 2 H, H-a), 7·40 (d, 4 H, H-b + H-d), 6·99 (d, 2 H, H-f), 4·06 (t, 2 H, OCH_2), 1·83 (m, 2 H, OCH_2CH_2), 1·50–1·21 [m, 18 H, $(CH_2)_9$], 0·90 (t, 3 H, CH_3). δ_C ($CDCl_3$, 75 MHz) 164·2, 163·8, 157·2, 156·4, 156·3, 155·5, 151·7, 149·3, 149·0, 139·4, 136·7, 136·6, 132·4, 131·8, 129·0, 128·7, 128·4, 127·1, 126·7, 123·7, 122·3, 122·1, 121·5, 121·0, 118·3, 117·4, 114·4, 68·4, 31·9, 29·6, 29·5, 29·3, 29·1, 25·9, 22·6, 14·0.

2.2.3. *Organopalladium complexes*

In a typical procedure a solution of [$Pd(PhCN)_2Cl_2$] [12] (0·09 mmol) in benzene ($4\,cm^3$) was transferred by cannula to a stirred suspension of the appropriate ligand in methanol ($4\,cm^3$). Stirring was continued at room temperature for 4–12 h depending on the ligand. The resulting pale yellow solid was recovered by filtration, washed with methanol and diethyl ether, and dried *in vacuo*.

2.2.3.1. *[Pd(L-6)Cl]*. Reaction time, 20 h. Yield, 98%. Found: C, 63·08; H, 4·37; N, 3·68. Calc. for

$C_{42}H_{35}ClN_2O_5Pd$: C, 63·89; H, 4·47; N, 3·55%. IR ν (Nujol mull)/cm^{-1} 1732 (COO). ^{1}H NMR δ_H ($CDCl_3$, 300 MHz) 8·51 (br d, 1 H, H-6), 8·02 (d, 1 H, H-3), 7·90 (ddd, 1 H, H-4), 7·74 (br s, 1 H, H-3′), 7·54 (dd, 1 H, H-3″ or H-6″), 7·31 (m, 1 H, H-5), 6·99 (br t, 1 H, H-4″ or H-5″), 6·92 (ddd, 1 H, H-5″ or H-4″). Other signals: δ 8·34 (d, 2 H, H-c), 8·17 (d, 2 H, H-e), 7·82 (d, 2 H, H-a), 7·42 (d, 4 H, H-b + H-d), 7·00 (d, 2 H, H-f), 4·07 (t, 2 H, OCH_2), 1·84 (m, 2 H, OCH_2CH_2), 1·59–1·34 [m, 6 H, $(CH_2)_3$], 0·93 (t, 3 H, CH_3).

2.2.3.2. *[Pd(L-8)Cl]*. Reaction time, 15 h. Yield, 90%. Found: C, 63·90; H, 4·61; N, 3·69. Calc. for $C_{44}H_{39}ClN_2O_5Pd$: C, 64·64; H, 4·81; N, 3·43%. IR ν (Nujol mull)/cm^{-1} 1733 (COO). ^{1}H NMR δ_H ($CDCl_3$, 300 MHz) 8·88 (br d, 1 H, H-6), 8·00 (m, 2 H, H-3 + H-4), 7·80 (br s, 1 H, H-3′), 7·79 (m, 1 H, H-3″ or H-6″), 7·70 (s, 1 H, H-5′), 7·53 (m, 1 H, H-5), 7·29 (m, 1 H, H-6″ or H-3″), 7·11 (m, 2 H, H-4″ + H-5″). Other signals: 8·32 (d, 2 H, H-c), 8·17 (d, 2 H, H-e), 7·82 (d, 2 H, H-a), 7·46 (d, 2 H, H-d), 7·42 (d, 2 H, H-b), 7·00 (d, 2 H, H-f), 4·06 (t, 2 H, OCH_2), 1·84 (m, 2 H, OCH_2CH_2), 1·49–1·25 [m, 10 H, $(CH_2)_5$], 0·90 (t, 3 H, CH_3).

2.2.3.3. *[Pd(L-12)Cl]*. Reaction time, 20 h. Yield, 70%. Found: C, 65·78; H, 5·29; N, 3·22. Calc. for $C_{48}H_{47}ClN_2O_5Pd$: C, 65·98; H, 5·42; N, 3·21%. IR ν (Nujol mull)/cm^{-1} 1733 (COO). ^{1}H NMR δ_H ($CDCl_3$, 300 MHz) 8·62 (br d, 1 H, H-6), 8·03 (d, 1 H, H-3), 7·94 (br t, 1 H, H-4), 7·77 (br s, 1 H, H-3′), 7·63 (br d, 1 H, H-3″ or H-6″), 7·52 (br s, 1 H, H-5′), 7·39 (m, 1 H, H-5), 7·31 (br d, 1 H, H-6″ or H-3″), 7·05–6·96 (m, 2 H, H-4″ + H-5″). Other signals: 8·34 (d, 2 H, H-c), 8·17 (d, 2 H, H-e), 7·82 (d, 2 H, H-a), 7·44 (d, 2 H, H-d), 7·41 (d, 2 H, H-b), 7·00 (d, 2 H, H-f), 4·07 (t, 2 H, OCH_2), 1·84 (m, 2 H, OCH_2CH_2), 1·49–1·25 [m, 10 H, $(CH_2)_9$], 0·89 (t, 3 H, CH_3).

3. Results and discussion

3.1. *Synthesis and photophysical studies*

The synthetic procedure followed to achieve the tridentate HL-*n* ligands is shown in the scheme. Two major steps are required to assemble the different parts of the molecules. Formation of the functional 2,2′-bipyridine skeleton is accomplished in the first step through a Kröhnke synthesis [17]. Intermediate **1**, which bears a hydroxy group, is now suitable for condensation with the acid **2-*n*** prepared by standard methods. Grafting of the 4-(4-alkoxybenzoyloxy)benzoyl mesogenic moiety to **1** can be carried out in the presence of DCC and catalytic amounts of PPy [18]. The resulting diester ligands—white solids with a high solubility in common, non-protic organic solvents—were obtained in pure form in low yield (25–40%) after several recrystallizations at low temperature (−20°C).

Organopalladium [Pd(L-*n*)Cl] species were readily produced under mild conditions. Conversion to the pale yellow cyclometallated products was achieved in fairly high yield provided that the reaction time was above 12 h. ^{1}H NMR spectroscopy has been rather effective in assessing the *C*,*N*,*N*-bonding mode shown by the deprotonated L-*n* ligands. Since the free phenyl ring AA′MM′*X* spin system of HL-*n* changes to an ABM*X* spin system upon metallation, the assignment is straightforward. In general, proton NMR patterns for the co-ordinated 6′-phenyl-2,2′-bipyridine moiety were similar to that seen for the related palladium complex with the non-substituted 6′-phenyl-2,2′-bipyridine ligand [19]. Further proof of metallation at the C-2″ position by ^{13}C NMR spectroscopy was hampered by the poor solubility of the [Pd(L-*n*)Cl] species.

The absorption spectra and luminescence properties of all the HL-*n* ligands are similar, as is the case for the metal complexes. Therefore, as typical representative examples of this family of compounds we will discuss in detail only the absorption and luminescence properties of the free ligand HL-12 and [Pd(L-12)Cl].

The absorption spectrum of HL-12 in dichloromethane solution is dominated by an intense band peaking at 272 nm ($\varepsilon = 84\,000$ M^{-1} cm^{-1}), followed by a less intense band at lower energies, with a shoulder at 315 nm ($\varepsilon = 11\,600$ M^{-1} cm^{-1}). Because of their intensities and similarity to the absorption bands of other polypyridine ligands [20], both the bands are attributed to spin-allowed π–π* transitions involving the polypyridine framework. The absorption spectrum of [Pd(L-12)Cl] in dichloromethane is quite similar to that of the free ligand, exhibiting an intense band at 295 nm ($\varepsilon = 56\,300$ M^{-1} cm^{-1}) followed by a less intense band peaking at 332 nm ($\varepsilon = 18\,000$ M^{-1} cm^{-1}). The slight red-shifts of the bands on passing from the free ligand to the metal complex suggest that the bands dominating the absorption spectrum of the complex can be attributed to metal-perturbed ligand-centred (*LC*) spin-allowed transitions [2].

HL-12 exhibits an intense luminescence both at room temperature in dichloromethane solution ($\lambda_{max} = 360$ nm, $\Phi = 0{\cdot}24$) and in a rigid butyronitrile matrix at 77 K ($\lambda_{max} = 362$ nm). Under both of the above experimental conditions, the emission band is narrow and unstructured and the luminescence decay is biexponential (fluid solution at room temperature: $\tau_1 = 1{\cdot}2$ ns, $\tau_2 = 90$ ns; rigid matrix at 77 K: $\tau_1 = 0{\cdot}6$ ns, $\tau_2 = 5{\cdot}2$ ns). On the basis of the emission energy, lifetimes and quantum yields, the luminescence of HL-12 is attributed to π–π* fluorescence in all cases.

[Pd(L-12)Cl] exhibits luminescence in a rigid butyronitrile matrix at 77 K. The emission spectrum is structured, with maxima at 476 and 508 nm (figure 3). The luminescence decay is mono-exponential, giving a luminescence lifetime of 110 μs. On the basis of the emission energy and lifetime and of the vibrational progression of the emission spectrum (about 1300 cm^{-1}, suggesting that the dominating acceptor mode is the C=C and/or C=N stretching mode of the polypyridine framework), the luminescence is attributed to a formally triplet metal-perturbed *L C* excited state. The luminescence spectrum and lifetime are typical of *L C* emission from polypyridine metal complexes [20], including Pd(II) cyclometallated compounds [21]. At room temperature, the luminescence is quenched in fluid dichloromethane solution, as is usual for Pd(II) cyclometallated species, possibly because of non-radiative deactivation by the thermal population of a low-lying metal-centred level [21, 21]. On the other hand, a microcrystalline sample of the complex exhibits a structured luminescence at room temperature (maxima at 430 and 450 nm), which can also be safely attributed to the same $^3L\,C$ level responsible for the 77 K emission. There is no evidence for excimer or metal–metal bonded dimeric emissions sometimes found in square-planar metal complexes [22]. This indicates that intermolecular interactions in the solid state are not strong enough to perturb the excited state properties of the 'isolated' molecules in [Pd(L-12)Cl].

3.2. *Mesomorphism*

The mesomorphic properties of both ligands and complexes were investigated by DSC and thermal polarizing optical microscopy. Variable-temperature X-ray diffraction was also instrumental in confirming the nature of the polymorphism exhibited by the HL-*n* molecules. Transition temperatures and phase assignments are listed in table 1.

All HL-*n* ligands are nematogens with a mesomorphic range decreasing as *n* increases. Since melting temperatures decrease only slightly with increasing *n*, the reduction in mesomorphic range is associated mainly with the lowering of the clearing point.

Optical textures for HL-*n* were best seen by slow cooling of the isotropic melt. A typical schlieren texture appears first, which immediately gives way to a marbled texture. As confirmed by DSC, besides the nematic phase all ligands show two crystal phases, at least in the first heating run. Thus, the thermogram of a pristine sample of HL-6 shows a crystal–crystal transition at 110°C followed by an incipient crystal–nematic transition at 140°C. However, the latter transition occurs simultaneously with a recrystallization process (clearly observed by optical microscopy) and the definitive crystal–nematic transition is seen at 159·7°C. Subsequent heating runs showed only the crystal–nematic transition at 141·0°C, as given in table 1. The clearing transition is always observed at 173·0°C.

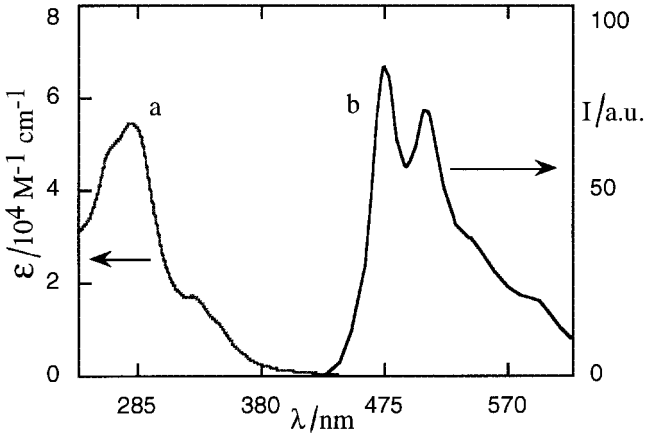

Figure 3. Absorption spectrum for fluid dichloromethane solution at 298 K (a) and luminescence spectrum for rigid butyronitrile matrix at 77 K (b) of [Pd(L-12)Cl].

Table 1. Mesomorphic behaviour of free diester ligands HL-*n* and organopalladium [Pd(L-*n*)Cl] species. Cr, crystal; N, nematic; I, isotropic liquid; Sm, smectic.

Compound	Transition	*T*/°C[a]	Δ*H*/kJ mol^{-1} [a]
HL-6	Cr–N	141·0	21·2
	N–I	173·0	0·40
	I–N	171·4	−0·34
	N–Cr	100·1	−18·1
HL-8	Cr–N	140·0	44·2
	N–I	162·2	0·60
	I–N	161·1	−0·50
	N–Cr	11·3	−39·1
HL-12	Cr–Cr′	95·8	4·0
	Cr′–N	131·2	34·4
	N–I	144·7	0·6
	I–N	142·4	−0·5
	N–Cr	89·2	−5·8
[Pd(L-6)Cl]	Cr–I	313·3	45·0
	I–N	275[b]	
	N–Cr	200[b]	
[Pd(L-8)Cl]	Cr–I	306·0	45·0
	I–N	271[b]	
	N–Cr	213[b]	
[Pd(L-12)Cl]	Cr–I	274·3	33·2
	I–SmA	257[b]	
	SmA–Cr	212[b]	

[a] Data from the second (HL-*n* ligands) or the first (complexes) DSC cycle.
[b] Data from optical microscopy.

Whereas both HL-8 and HL-12 undergo a crystal–crystal transition in the first heating run, only for HL-12 is this transition maintained in the subsequent heating cycles. The DSC thermogram of HL-12 is also unique, as the recrystallization peak in the cooling scan is rather weak.

Figures 4 and 5 show the XRD spectra of HL-6 as a function of temperature in the first and second thermal cycle, respectively. Although the quality of the room temperature (RT) crystal phase of the pristine sample is rather poor (figure 4, A), a lamellar structure characterized by a layer spacing $d = 39{\cdot}8$ Å is apparent. The above diffraction pattern remains unaffected until a crystal–crystal phase transition occurs at ≈ 110°C (figure 4, B), which corresponds to the loss of the lamellar structure of the solid phase. A further temperature increase shows the formation of the nematic phase above 160°C (figure 4, C) which persists up to the isotropization temperature (figure 4, D). The small angle diffuse signal centred at about 3·5°, and associated with the nematic short range order, was seen only with the sample aligned in the external magnetic field. The 'apparent molecular length' (AML) derived from the position of this diffuse signal is $d \approx 27{\cdot}2$ Å. Given the calculated value $L = 31{\cdot}8$ Å for the length of the molecule in the fully extended conformation, the above value of d corresponds to an average tilt angle $\langle \beta \rangle = \cos^{-1}(d/L) \approx 31°$, which is comparable to the average tilt angle (20–30°) that is normally found in low-molar mass nematics [23]. On cooling from the isotropic melt the nematic mesophase appeared below 171°C (figure 4, E) and persisted down to 110°C where a nematic–crystal transition was observed (figure 4, F). As shown in figure 4, G, the lamellar structure of the r.t. solid phase is regained after one thermal cycle and, in agreement with DSC and optical microscopy observations, further heating showed only the crystal–nematic transition (figure 5).

A similar XRD sequence was observed for sample HL-8. The r.t. solid phase has a relatively poor crystalline quality and a lamellar structure with a d spacing of 45·1 Å. The high-temperature solid phase (which appears above 100°C) has a better crystalline quality and a persistent lamellar structure, although with a reduced d spacing (37·7 Å). In agreement with the increased length of the molecule, the AML in the nematic phase was found to be 29·0 Å. Again, the r.t. solid phase after one thermal cycle exhibits a lamellar structure ($d = 53{\cdot}3$ Å) which is maintained in the subsequent heating cycle up to the crystal–nematic transition.

Different behaviour was observed for sample HL-12 for which the crystal–crystal transition was seen during all the heating cycles. While the crystal quality is notably different, the lamellar spacing is essentially the same in both solid phases ($d = 28{\cdot}8$ Å). The observed AML in the nematic phase is 33·0 Å. In addition, the XRD spectra in the cooling cycles show the occurrence of

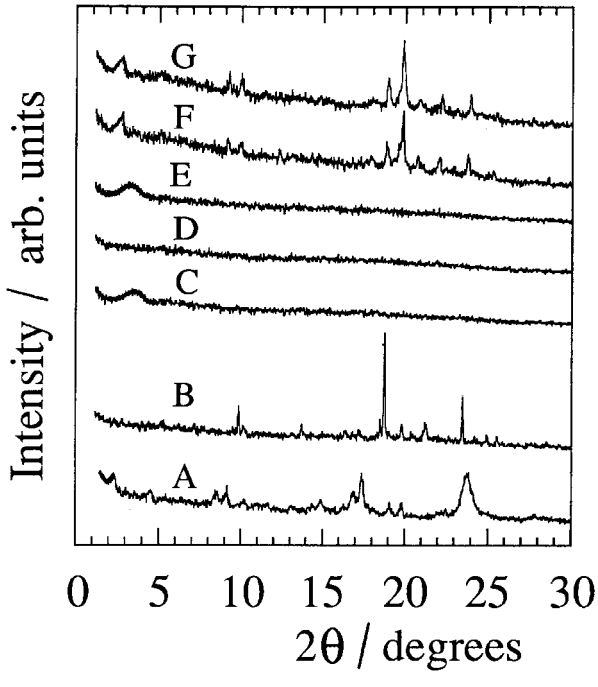

Figure 4. XRD spectra of HL-6 recorded at different temperatures in the first thermal cycle. Heating: (A) $T = 25$°C; (B) $T = 110$°C; (C) $T = 165$°C; (D) $T = 180$°C. Cooling: (E) $T = 160$°C; (F) $T = 100$°C; (G) $T = 25$°C.

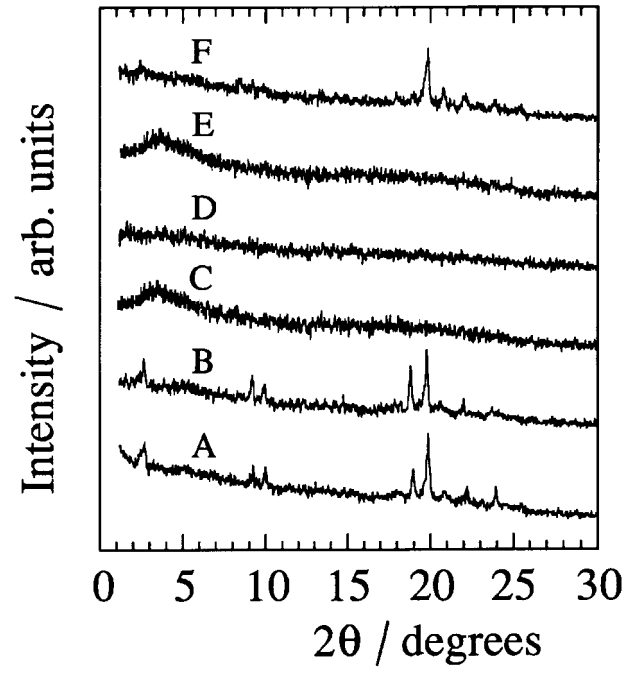

Figure 5. XRD spectra of HL-6 recorded at different temperatures in the second thermal cycle. Heating: (A) $T = 25$°C; (B) $T = 110$°C; (C) $T = 150$°C; (D) $T = 180$°C. Cooling: (E) $T = 160$°C; (F) $T = 100$°C; (G) $T = 25$°C.

partial recrystallization below 90°, which results in the formation of a solid phase with a partially amorphous nature.

Whereas no regularity of the trend for the lamellar solid phase spacing is observed along the series HL-*n*, a regular increase of AML with *n* in the nematic phase is apparent, in agreement with the lengthening of the molecule. The constancy of the AML/*L* ratio (table 2) is consistent with the constancy of the average tilt angle in the nematic phase.

The metallated species [Pd(L-*n*)Cl] show monotropic behaviour and their mesomorphism was studied by DSC and optical microscopy. Melting temperatures are rather high and slight decomposition around the crystal–isotropic transition is the undesired outcome. Despite this latter problem, optical textures are clearly seen on cooling from the isotropic liquid. The two lower homologues show nematic behaviour and give either a schlieren texture ([Pd(L-6)Cl]) or nematic droplets followed by the schlieren texture ([Pd(L-8)Cl]). In both cases, the large birefringent domains alternate with smaller optically isotropic regions. In [Pd(L-12)Cl] the nematic mesomorphism of the lower homologues is replaced by smectic mesomorphism. A well defined fan-shaped texture with focal conics is observed which is typical of a smectic A phase. This assignment seems to be confirmed by the occurrence of bâtonnets just before the above texture starts to grow.

As a general trend, the solidification of metal-containing species is always slow and partial, resulting in weak and diffuse DSC features.

4. Conclusion

HL-*n* ligands do not represent the only known example of mesomorphic 2,2′-bipyridine derivatives. The remarkable co-ordination chemistry of bipyridine ligand has recently drawn the attention of different groups of workers, although different goals were targeted [24–26]. More recently, Bruce and Rowe [27] synthesized both 4,4′- and 5,5′-diesters of 2,2′-bipyridine in order to prepare metallomesogens with high co-ordination numbers. The best candidates for complexation were the 5,5′-derivatives, which contained either four or six aromatic rings in the core of the mesogen. However, only the six-ring 2,2′-bipyridines gave mesomorphic complexes [28]. An intriguing report by Douce *et al.* has also appeared, describing a series of mesomorphic 5-methyl-5′-(4-*n*-alkoxyphenylvinyl)-2,2′-bipyridines [29]. The stilbene chromophore had been introduced with the aim of generating ordered luminescent metal complexes. A strong luminescence was indeed observed for the synthesized bipyridines, but to the best of our knowledge no report of the planned metal derivatives has yet appeared.

Table 2. XRD data for HL-*n* in the nematic phase.

Compound	AML/Å[a]	*L* /Å[b]	$\langle\beta\rangle$/°[c]
HL-6	27·2	31·8 ± 1	31·0 ± 3
HL-8	29·0	34·0 ± 1	31·5 ± 3
HL-12	33·0	39·0 ± 1	32·0 ± 2·5

[a] Apparent molecular length in the nematic phase.
[b] Calculated value for a fully extended molecule.
[c] Average tilt angle in the aligned nematic phase.

We have been successful in synthesizing mesomorphic ligands which to some extent retain mesomorphism on complexation. The ligands are nematogens with a rather small mesomorphic range (14–32°C) and, while the melting point is scarcely affected by the chain length, a destabilization of the nematic phase occurs with increasing chain length. Metal co-ordination promotes a dramatic stabilization of the crystal phase and reasons for this behaviour may lie in particulary strong dipolar interactions. These are increased both by the *cisoid* conformation of the chelating bipyridine fragment and the introduction of a polar M–Cl bond on one side of the molecule. A further contribution to the crystal phase stabilization may arise from weak intra-ligand stacking arising from the formation of a planar cyclometallated core. As a result, the mesophase becomes metastable and it occurs only on cooling from the melt. Increasing values of the chain length lower the melting temperature as well as promoting more ordered mesophases. Thus, the nematic phase seen for [Pd(L-6)Cl] and [Pd(L-8)Cl] is lost for [Pd(L-12)Cl] in favour of a smectic A phase.

The remarkable luminescence properties of both ligand HL-*n* and complexes in solution and in the solid state have been studied. Although the results are not unexpected and closely match those obtained for palladium cyclometallated species [11, 21], our initial expectation of achieving both mesomorphic and luminescent metal complexes has been partially fulfilled. This is the first time that calamitic metallomesogens have been designed to display photophysical properties [30], yet the materials we have prepared are not ideal candidates for photophysical studies on the mesomorphic state [31, 32] (i.e. they are monotropic, suffer from decomposition at the clearing point, and are mesomorphic at rather high temperatures).

At present, luminescence and mesomorphism are therefore displayed under different conditions. An alternative synthetic strategy must be devised to improve the mesogenic character of the species, making them more attractive and suitable for photophysical studies of the liquid crystalline state.

Financial support from the Italian Ministero dell'Università e della Ricerca Scientifica e Tecnologica (MURST) and Consiglio Nazionale delle Ricerche (CNR) is gratefully acknowledged.

References

[1] Serrano, J. L. (editor), 1996, *Metallomesogens* (Weinheim: VCH).

[2] Bruce, D. W., 1992, in *Inorganic Materials*, edited by D. W. Bruce and D. O'Hare (Chichester: John Wiley), Chap. 8.

[3] (*a*) Giroud-Godquin, A.-M., and Maitlis, P. M., 1991, *Angew. Chem. int. Ed. Engl*., **30,** 375; (*b*) Espinet, P., Esteruelas, M. A., Oro, L. A., Serrano, J. L., and Sola, E., 1992, *Coord. Chem. Rev*., **117,** 215; (*c*) Hudson, S. A., and Maitlis, P. M., 1993, *Chem. Rev*., **83,** 861; (*d*) Polishchuk, A. P., and Timofeeva, T. V., 1993, *Russ. chem. Rev*., **62,** 291; (*e*) Oriol, L., and Serrano, J. L., 1995, *Adv. Mater*., **7,** 348; (*f*) Neve, F., 1996, *Adv. Mater*., **8,** 277.

[4] Gray, G. W., Harrison, K. J., and Nash, J. A., 1973, *Electron. Lett*., **9,** 130.

[5] Bruce, D. W., Lalinde, E., Styring, P., Dunmur, D. A., and Maitlis, P. M., 1986, *J. chem. Soc. chem. Commun*., 581.

[6] (*a*) Lattermann, G., Schmidt, S., Kleppinger, R., Wendorff, J. H., 1992, *Adv. Mater*., **4,** 30; (*b*) Schmidt, S., Lattermann, G., Kleppinger, R., and Wendorff, J. H., 1994, *Liq. Cryst*., **16,** 693.

[7] Serrette, A. G., and Swager, T. M., 1994, *Angew. Chem. int. Ed. Engl*., **33,** 2342.

[8] (*a*) Lai, C. K., Serrette, A. G., and Swager, T. M., 1992, *J. Am. chem. Soc*., **114,** 7948; (*b*) Serrette, A. G., Lai, C. K., and Swager, T. M., 1994, *Chem. Mater*., **6,** 2252.

[9] Holbrey, J. D., Tiddy, G. J. T., and Bruce, D. W., 1995, *J. chem. Soc. Dalton Trans*., 1769.

[10] Neve, F., Ghedini, M., and Crispini, A., 1996, *Chem. Commun*., 2463.

[11] Neve, F., Crispini, A., and Campagna, S., 1997, *Inorg. Chem*., **36,** 6150.

[12] Treffert-Ziemelis, S. M., Golus, J., Strommen, D., and Kincaid, J. R., 1993, *Inorg. Chem*., **32,** 3890.

[13] Karash, M. S., Seyler, R. C., and Mayo, F. R., 1938, *J. Am. chem. Soc*., **60,** 882.

[14] Demas, J. N., and Crosby, G. A., 1971, *J. phys. Chem*., **75,** 991.

[15] Dawson, W. R., and Windsor, M. W., 1968, *J. phys. Chem*., **72,** 3251.

[16] Neve, F., Ghedini, M., Levelut, A.-M., and Francescangeli, O., 1994, *Chem. Mater*., **6,** 70.

[17] Kröhnke, F., 1976, *Synthesis*, 1.

[18] Hassner, A., and Alexanian, V., 1978, *Tetrahedron Lett*., 4475.

[19] Constable, E. C., Henney, R. P. G., Leese, T. A., and Tocher, D. A., 1990, *J. chem. Soc. Dalton Trans*., 443.

[20] Juris, A., Balzani, V., Barigelletti, F., Campagna, S., Belser, P., and von Zelewsky, A., 1988, *Coord. Chem. Rev*., **84,** 85.

[21] Maestri, M., Balzani, V., Deuschel-Cornioley, C., and von Zelewsky, A., 1992, *Adv. Photochem*., **17,** 1 and refs therein.

[22] Moulding, V. H., and Miskowski, V. M., 1991, *Coord. Chem. Rev*., **111,** 145.

[23] De Vries, A., Ekachai, A., and Speilberg, N., 1979, *Mol. Cryst. liq. Cryst*., **49,** 143.

[24] Hanabusa, K., Higashi, J.-I., Koyama, T., Shira, H., Hojo, N., and Kurose, A., 1989, *Makromol. Chem*., **190,** 1.

[25] Bruce, D. W., Holbrey, J. D., Tajbakhsh, A. R., and Tiddy, G. J. T., 1993, *J. mater. Chem*., **3,** 905.

[26] Kuboki, T., Araki, K., Yamada, M., and Shiraishi, S., 1994, *Bull. chem. Soc. Jpn*., **67,** 984.

[27] (*a*) Bruce, D. W., and Rowe, K. E., 1995, *Liq. Cryst*., **18,** 161; (*b*) Rowe, K. E., and Bruce, D. W., 1996, *Liq. Cryst*., **20,** 183.

[28] Rowe, K. E., and Bruce, D. W., 1996, *J. chem. Soc. Dalton Trans*., 3913.

[29] Douce, L., Ziessel, R., Seghrouchni, R., Skoulios, A., Campillos, E., and Deschenaux, R., 1995, *Liq. Cryst*., **18,** 157.

[30] Ghedini, M., Pucci, D., Calogero, G., and Barigelletti, F., 1997, *Chem. Phys. Lett*., **267,** 341.

[31] Weiss, R. G., 1991, in *Photochemistry in Organized and Constrained Media*, edited by V. Ramamurthy (Weinheim: VCH), pp. 603–690.

[32] Chen, S. H., Shi, H., Conger, B. M., Mastrangelo, J. C., and Tsutsui, T., 1996, *Adv. Mater*., **8,** 998.